THE PUBLISHING HOUSE
OF THE ROMANIAN ACADEMY

PROCEEDINGS OF THE ROMANIAN ACADEMY, Series A
Volume 24, Number 1/2023, pp. 35–42
DOI: 10.59277/PRA-SER.A.24.1.05

CIRCULAR GEODESICS IN MANNHEIM-KAZANAS SPACETIME

Vitalie LUNGU, Marina-Aura DARIESCU

"Alexandru Ioan Cuza University" of Iaşi, Faculty of Physics
Bd. Carol I, no. 11, 700506 Iaşi, Romania
Corresponding author: Marina-Aura DARIESCU, E-mail: marina@uaic.ro

Abstract. We investigate the null and timelike circular geodesics in Mannheim–Kazanas spacetime. The effective potential, circular orbits and their stability are discussed, in terms of Lyapunov exponent. The critical null and timelike geodesics are compared to the ones obtained in Schwarzschild's case. Finally, we focus on the black hole's thermodynamic properties.

Key words: conformal gravity, Mannhein-Kazanas metric, geodesics, black hole's heat capacity.

1. INTRODUCTION

As the dark matter problem is still unsolved, alternative theories to General Relativity (GR) have been proposed. Among these, the Conformal Gravity (CG) is a reliable candidate and, similarly to GR, it uses a metric to describe gravity as a curved spacetime [1]. One of the most promising solutions of CG is the Mannheim-Kazanas (MK) solution which, beside the Schwarzschild term, contains linear and quadratic contributions. The CG gives an answer to the problem of rotation curves of spiral galaxies, without the need of the dark sector [2]. The model has been tested on numerous galaxies, and provided fully acceptable results [3].

Since a detailed study of test particles in the MK spacetime might highlight its characteristics, the main part of this work is dedicated to the motion of particles in this manifold. It is assumed that the test particles orbit relatively close to the central black hole within the galactic disk. Thus, only the linear term in the metric is significant and one may neglect the quadratic one. For a comparison, we recommed the work [4], where the authors have used both terms to investigate the orbits of test particles in regions where the quadratic contribution acts like a perturbation of cosmological origin. Also, we assume that most of the galactic mass is enclosed in the central black hole [5]. In the following sections, the null and timelike circular geodesics are investigated, highlighting the stability of circular orbits in terms of the Lyapunov exponent. In the last part of the present work, we give some remarks on the black hole thermodynamics.

2. STRUCTURE OF THE MANNHEIM–KAZANAS SPACETIME

In this section, we introduce the so-called MK metric, which was obtained by Mannheim and Kazanas as an exact solution in Conformal Gravity [6]. For the line element:

$$\mathrm{d}s^2 = -g(r)\mathrm{d}t^2 + \frac{\mathrm{d}r^2}{g(r)} + r^2\left(\mathrm{d}\theta^2 + \sin^2\theta\,\mathrm{d}\varphi^2\right) \tag{1}$$

the metric function, in its original form, has the general expression [2, 6]:

$$g(r) = 1 - 3Ma - \frac{M\,(2-3Ma)}{r} + ar - br^2 \tag{2}$$

where M is the galaxy mass and a and b are integration constants.

The parameter a is a correction to the theory of general relativity, while b acts like a cosmological constant [6, 7]. One may observe that if we set $a = 0$, we obtain the de Sitter–Schwarzschild solution. The value of the parameter b is $9.54 \times 10^{-54}\,\mathrm{m}^{-2}$ and is constant for all galaxies. The parameter $a = a_0 + a_g$ has two components, namely $a_0 = 3.06 \times 10^{-28}\,\mathrm{m}^{-1}$ and $a_g = Na^*$, where $a^* = 5.42 \times 10^{-39}\,\mathrm{m}^{-1}$ and $N = M/M_{Sun}$ [3].

One may work in the approximation $3Ma \ll 1$ so that the metric function (2) can be written as:

$$g(r) = 1 - \frac{2M}{r} + ar - br^2 \tag{3}$$

and contains, besides the Schwarzschild expression, a linear and a quadratic contribution. Given the values of the parameters a and b, the linear term is significant in the galactic halo and can be taken as an universal constant independent of the galactic mass, while the quadratic term takes significance at cosmological distances [8]. This general case has been discussed in detail in [4].

Also, in (2), we notice a constant parameter in the metric function, of the form $1 - 3Ma$, which has been considered in [2]. This is leading to conical singularities and is affecting the general analysis, being connected to the mass parameter and to the cosmological constant.

In the followings, since we are interested in the motion of particles relatively close to the galactic center, we neglect the quadratic term and work with the simple expression

$$g(r) = 1 - \frac{2M}{r} + ar \tag{4}$$

which leads to an unique horizon

$$r_h = \frac{\sqrt{1+8Ma}-1}{2a} \tag{5}$$

For $8MA \ll 1$, this has the expression $r_h \approx 2M(1-4Ma)$, which is smaller than the Schwarzschild horizon.

3. GEODESICS IN THE MK SPACETIME

The aim of this section is to discuss the geodesics for both light rays and neutral particles. Let us start with the Lagrangian describing the MK spacetime [9]:

$$\mathscr{L} = -\frac{1}{2}\left[-g(r)\dot{t}^2 + \frac{\dot{r}^2}{g(r)} + r^2\left(\dot{\theta}^2 + \sin^2\theta\,\dot{\varphi}^2\right)\right], \tag{6}$$

where dot represents the derivative with respect to proper time τ.

As there are two Killing vectors, ∂_t and ∂_φ, one may identify two constants of motion, the energy E and the angular momentum L:

$$E = \frac{\mathrm{d}\mathscr{L}}{\mathrm{d}\dot{t}} = g(r)\dot{t} \tag{7}$$

$$L = \frac{\mathrm{d}\mathscr{L}}{\mathrm{d}\dot{\varphi}} = -r^2\sin^2\theta\,\dot{\varphi} \tag{8}$$

We may consider the motion in the equatorial plane without the loss of generality. This implies $\theta = \frac{\pi}{2}$ and

$\dot{\theta} = \ddot{\theta} = 0$. Under this condition and using the equations (7) and (8), the Lagrangian (6) becomes:

$$\mathscr{L} = -\frac{1}{2}\left(\frac{\dot{r}^2}{g(r)} + \frac{L^2}{r^2} - \frac{E^2}{g(r)}\right) \tag{9}$$

Henceforth, the equation of motion reads:

$$\dot{r}^2 + \left(\frac{L^2}{r^2} + k\right)\left(1 - \frac{2M}{r} + ar\right) = E^2, \tag{10}$$

with $2\mathscr{L} = k$, where $k = 0$ stands for null geodesics and $k = 1$ for the timelike ones. By comparing (10) with the equation of motion $\dot{r}^2 + V_{eff}(r) = E^2$, one may identify the expression of the effective potential:

$$V_{eff}(r) = \left(\frac{L^2}{r^2} + k\right)\left(1 - \frac{2M}{r} + ar\right) \tag{11}$$

In the force acting on particles:

$$F(r) = -\frac{1}{2}\frac{\mathrm{d}V_{eff}(r)}{\mathrm{d}r} = -\frac{1}{2}\left(\frac{2M}{r^2} + a\right)\left(\frac{L^2}{r^2} + k\right) + \left(1 - \frac{2M}{r} + ar\right)\frac{L^2}{r^3} \tag{12}$$

one may notice both attractive and repulsive contributions.

3.1. Circular null geodesics

For $k = 0$ and $L \neq 0$, the effective potential (11) reads:

$$V_{eff}(r) = \frac{L^2}{r^2}\left(1 - \frac{2M}{r} + ar\right) \tag{13}$$

and is represented in Fig. 1. The potential is zero for $r = r_h$ and $r \to \infty$. Due to the nature of the potential, the circular orbits close to the black hole are unstable [4].

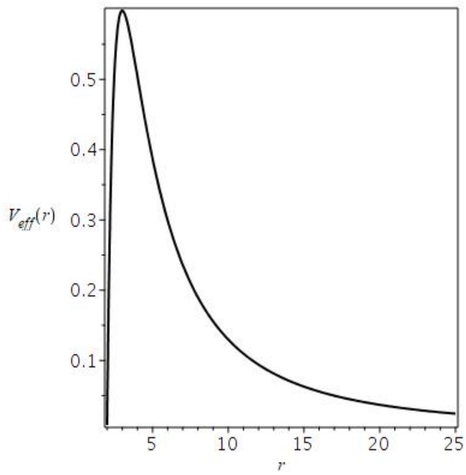

Fig. 1 – The effective potential (13), for $M = 1$, $L = 4$ and $a = 0.001$.

The particle's behavior depends on its energy E. A circular orbit implies $\dot{r}^2 = 0$, thus $E^2 = V_{eff}(r_c)$. From the condition

$$\frac{\mathrm{d}V_{eff}(r)}{\mathrm{d}r} = 0 \tag{14}$$

we get the radius of the circular orbit:

$$r_c = \frac{\sqrt{1+6Ma}-1}{a} > r_h \,. \tag{15}$$

One may observe that, for $6Ma \ll 1$, we recover the innermost circular orbit in the Schwarzschild case $r_c = 3M$. The last photon orbit which is also called the photon sphere [10] is located at $r = r_c$.

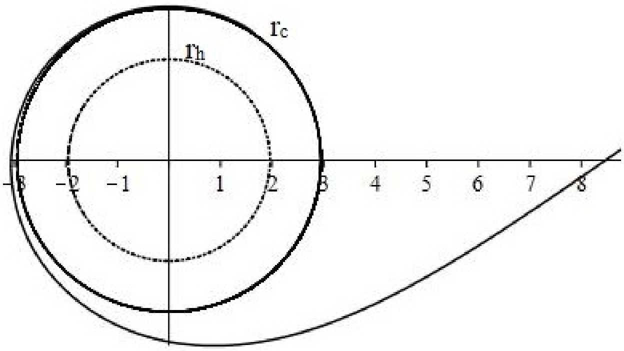

Fig. 2 – Critical null geodesic for $M = 1$, $a = 0.01$, $L = 2.22$ and $E = 0.446$.

In Fig. 2, is given a polar plot of the circular null geodesics for a particle arriving from a large r and settling into an unstable circular orbit at $r_c = 2.956$. The black hole's horizon is located at $r_h = 1.961$. Both the circular orbit and the black hole horizon are smaller than in the Schwarzschild case, due to the presence of the linear term in the metric function.

An important feature of the unstable circular orbits is the instability timescale defined as [11]

$$T(\lambda) = \frac{1}{\lambda} \tag{16}$$

where λ is the Lyapunov exponent [9, 11]

$$\lambda = \sqrt{-\left[\frac{g(r)^2}{2V_{eff}(r)}\frac{\mathrm{d}^2V_{eff}(r)}{\mathrm{d}r^2}\right]_{r=r_c}} \tag{17}$$

For the potential given in (13), this has the expression

$$\lambda = \frac{a\sqrt{\left(4Ma+1-\sqrt{6Ma+1}\right)\left(6Ma+1-\sqrt{6Ma+1}\right)}}{\left(\sqrt{6Ma+1}-1\right)^2} = \frac{\sqrt{(4M-r_c)(6M-r_c)}}{r_c^2} \tag{18}$$

To first order in Ma, the instability timescale reads

$$T(\lambda) \approx 3\sqrt{3}M\,(1-6Ma)\,.$$

In what it concerns the dependence of $T(\lambda)$ on the mass M, with λ given in (18), this rapidly increases with M, is reaching a maximum and then is slowly decreasing. In comparison, in the Schwarzschild case, the instability timescale of the circular null geodesics increases linearly with the black hole's mass. Let us mention that, in the MK metric, the parameter a depends on mass and as the mass increases, the linear term in the metric becomes more dominant.

3.2. Circular timelike geodesics

Let us focus now on the circular motion of massive particles. In this case, the effective potential is given in (11), with $k = 1$. As it can be seen in the figure 3, this potential remains above the effective potential in the Schwarzschild case.

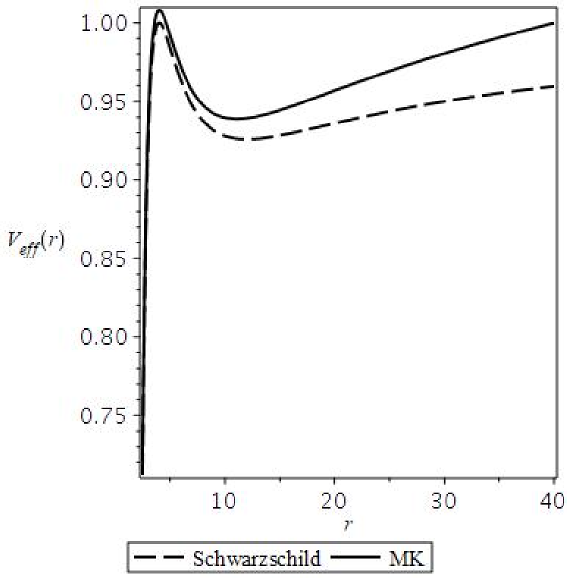

Fig. 3 – The effective potential (11), with $k = 1$. Here $M = 1$, $L = 4$ and $a = 0.001$.

By expanding the expression (12), one obtains the effective force

$$F(r) = -\frac{3ML^2}{r^4} - \frac{M}{r^2} - \frac{a}{2} + \frac{L^2}{r^3} + \frac{aL^2}{2r^2} \tag{19}$$

where the first three terms are attractive, while the last two terms are repulsive.

For the given values of M, L and a, there are two circular orbits, one at $r_{c1} = 4$ which is unstable due to the nature of the potential and the another one, at $r_{c2} = 11.075$, which is the innermost stable circular orbit. For distances $r > r_{c2}$, the circular orbits are stable as the force is attractive [2]. Both cases are shown in Fig. 4.

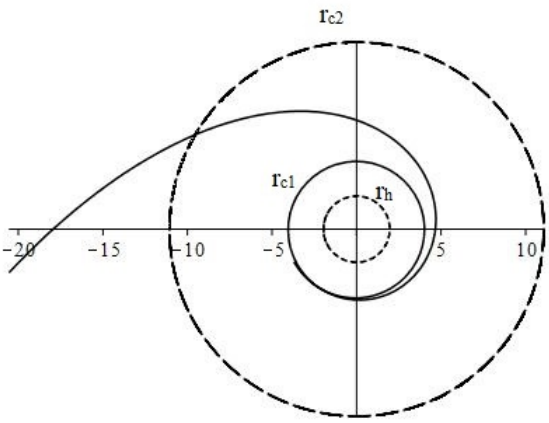

Fig. 4 – Critical timelike geodesic at $r = r_{c1}$ for $M = 1$, $a = 0.01$, $L = 4.02$ and $E = 1.00$. At $r = r_{c2}$, there is the innermost stable orbit.

At the end of this section, let us derive the constrains for the energy and angular momentum of a particle moving on a circular orbit. By introducing the notation $r = 1/u$, Eq. (10) becomes:

$$-\left(\frac{\mathrm{d}u}{\mathrm{d}\varphi}\right)^2 = \left(u^2 + \frac{1}{L^2}\right)\left(1 - 2Mu + \frac{a}{u}\right) - \frac{E^2}{L^2} = Y(u)\,. \tag{20}$$

The conditions for a circular orbit to occur are $Y(u = u_c) = 0$ and $Y'(u = u_c) = 0$. These are leading to the value of the energy and of the angular momentum as functions of u_c, M and a:

$$E^2 = \frac{2\left(2Mu_c^2 - a - u_c\right)^2}{u_c\left(-6Mu_c^2 + a + 2u_c\right)} \tag{21}$$

$$L^2 = \frac{2Mu_c^2 + a}{u_c^2\left(-6Mu_c^2 + a + 2u_c\right)}\,. \tag{22}$$

To have a physical orbit, the condition $-6Mu_c^2 + a + 2u_c > 0$ must hold and this leads to the constraint

$$r_c > \frac{\sqrt{1 + 6Ma} - 1}{a}\,.$$

It emerges naturally that the innermost circular orbit for timelike geodesics is larger than the innermost circular orbit of null geodesics. In view of these results, the Lyapunov exponent calculated in terms of M, a and r_c reads

$$\lambda = \sqrt{-\frac{a^2}{2} + \frac{6Ma}{r_c^3} - \frac{3a}{2r_c} + \frac{6M^2}{r_c^4} - \frac{M}{r_c^3}}\,, \tag{23}$$

where r_c can be derived from (20).

4. KLEIN-GORDON EQUATION AND THE EIKONAL APPROXIMATION

The transition between particles moving along timelike or null geodesics and the Klein-Gordon equation can be done in the eikonal limit, where the effective potential corresponding to the null geodesics should be the same with the one in the Klein-Gordon equation written in the Schrödinger-like form.

The Klein-Gordon equation for the particle of mass μ has the general expression

$$\frac{1}{r^2}\frac{\partial}{\partial r}\left[r^2 g(r)\frac{\partial \Psi}{\partial r}\right] + \frac{1}{r^2\sin\theta}\frac{\partial}{\partial\theta}\left[\sin\theta\frac{\partial\Psi}{\partial\theta}\right] + \frac{1}{r^2\sin^2\theta}\frac{\partial^2\Psi}{\partial\varphi^2} - \frac{1}{g(r)}\frac{\partial^2\Psi}{\partial t^2} - \mu^2\Psi = 0 \tag{24}$$

which has been analyzed in detail in [4]. With the variables separation

$$\Psi = R(r)Y_\ell^m(\theta,\varphi)\,e^{-i\omega t} \tag{25}$$

where Y_ℓ^m are the spherical functions, the radial equation reads

$$\frac{1}{r^2}\frac{\mathrm{d}}{\mathrm{d}r}\left[r^2 g(r)\frac{\mathrm{d}R}{\mathrm{d}r}\right] + \left[\frac{\omega^2}{g(r)} - \frac{\ell(\ell+1)}{r^2} - \mu^2\right]R = 0\,. \tag{26}$$

One may notice that, with the change of function $R(r) = F(r)/r$, and using the tortoise coordinate

$$\frac{\mathrm{d}r_*}{\mathrm{d}r} = \frac{1}{g(r)}$$

the radial equation gets the Schrödinger-like expression

$$\frac{\mathrm{d}^2F}{\mathrm{d}r_*^2}+\left\{\omega^2-g(r)\frac{l(l+1)}{r^2}-\frac{1}{2r}\frac{\mathrm{d}}{\mathrm{d}r}\left[g(r)^2\right]\right\}F=0\,. \tag{27}$$

In the eikonal approximation, i.e. large values of l, this turns into the simple expression

$$\frac{\mathrm{d}^2F}{\mathrm{d}r_*^2}+\left[\omega^2-g(r)\frac{l^2}{r^2}\right]F=0$$

where one may notice the same potential as the one given in (13).

5. REMARKS ON THE BLACK HOLE THERMODYNAMICS IN MK SPACETIME

In this section, we are going to compute the black hole's temperature and heat capacity as functions on its horizon. The black hole mass expressed in terms of the horizon reads:

$$M=\frac{1}{2}r_h\left(1+ar_h\right) \tag{28}$$

while the temperature is given by the expression

$$T=\frac{1}{4\pi}\left.\frac{\mathrm{d}g_{00}}{\mathrm{d}r}\right|_{r=r_h}=\frac{1+2ar_h}{4\pi r_h} \tag{29}$$

When $a=0$, we obtain the Hawking temperature for the Schwarzschild black hole $T_S=\dfrac{1}{8\pi M}$ [12].

The specific heat of the black hole on the horizon is defined as

$$C=\frac{\mathrm{d}M}{\mathrm{d}T}=\frac{\mathrm{d}M}{\mathrm{d}r_h}\left(\frac{\mathrm{d}T}{\mathrm{d}r_h}\right)^{-1} \tag{30}$$

and, in view of the equations (28) and (29), it has the form

$$C=-2\pi r_h^2\left(1+2ar_h\right)\approx-8\pi M^2\left(1-4a^2M^2\right), \tag{31}$$

where r_h is given in (5) and we have taken $8aM\ll 1$. The heat capacity is a negative quantity, meaning that we are dealing with a thermodynamically unstable black hole [13]. The absolute value of the heat capacity is smaller than in the Schwarzschild case ($C=-8\pi M^2$) and it is strongly depending on the mass of the black hole, as expected. Once the temperature of the black hole is obtained, the horizon and the Lyapunov exponent can be written in terms of T.

6. CONCLUSIONS

In the last years, the metric proposed by Mannheim and Kazanas has been intensively investigated and most of the papers are focusing on how the results provided by the MK model fit the available data on universally flat galaxies rotation curves. In what it concerns different types of geodesics, their stability and the connection to the Klein–Gordon equation in the eikonal limit, these were not investigated in detail and from this point of view the results obtained in the present paper are quite new. Such investigations have been done mainly for the Schwarschild black hole surrounded by quintessence [9, 14]. However, even though the metric function looks very similar, the change of sign in front of the linear term leads to an additional cosmological horizon which has a deep influence on the whole analysis.

The results derived in the present paper can be compared to the ones obtained in the alternative study [2], where the possible orbits in conformal spacetime has been discussed by solving the geodesics equations in terms of Weierstrass elliptic functions and derivatives of Kleinian sigma functions.

Since the orbits of test particles are close to the central black hole, we have worked with the simple expression (4) and we have derived the corresponding geodesics equation, as well as the potential and effective force acting on test particles. Due to the nature of the effective potential represented in Fig. 1, in the case of null geodesics, the circular orbits close to the black hole are unstable. The innermost circular orbit is represented in Fig. 2 and its instability timescale increases with the galactic center's mass. As expected, in the eikonnal approximation, the Klein-Gordon equation leads to the same effective potential (13).

For timelike geodesics, the potential remains above the Schwarzschild potential (Fig. 3) and it has a minimum outside the horizon implying the existence of a stable circular orbit. The innermost circular orbit in this case is larger than the innermost circular orbit of null geodesics and the Lyapunov exponent is given in (23).

Finally, we have derived the heat capacity which, similarly to the Schwarzschild case, is negative, pointing out an unstable black hole. The thermodynamic properties have been discussed $a \approx a_0$, i.e. for galaxies whose masses are $M \ll 10^{10} M_{Sun}$.

Let us mention that if one changes the sign of the linear term, it obtains metric functions describing the Schwarzschild black hole immersed in dark matter. The corresponding effective potential and the Klein-Gordon equation have been discussed in [14].

REFERENCES

1. K. HORNE, *Conformal gravity rotation curves with a conformal Higgs halo*, Monthly Notices of the Royal Astronomical Society, **458**, *4*, pp. 4122–4128, 2016.
2. B. HOSEINI, R. SAFFARI, S. SOROUSHFAR, *Study of the geodesic equations of a spherical symmetric spacetime in conformal Weyl gravity*, Classical and Quantum Gravity, **34**, *5*, art. 055004, 2017.
3. P. MANNHEIM, J. O'BRIEN, *Fitting galactic rotation curves with conformal gravity and a global quadratic potential*, Physical Review D, **85**, *12*, art. 124020, 2012.
4. M.A. DARIESCU, C. DARIESCU, *On the Mannheim Kazanas Solution*, Astrophysics and Space Science, **366**, *5*, art. 44, 2021.
5. J. O'BRIEN, T. CHIARELLI, P. MANNHEIM, *Universal properties of galactic rotation curves and a first principles derivation of the Tully-Fisher relation*, Physics Letters B, **782**, pp. 433–439, 2018.
6. P. MANNHEIM, D. KAZANAS, *Exact vacuum solution to conformal Weyl gravity and galactic rotation curves*, The Astrophysical Journal, **342**, pp. 635–649, 1989.
7. P. MANNHEIM, D. KAZANAS, *Solutions to the Reissner-Nordström, Kerr, and Kerr-Newman problems in fourth-order conformal Weyl gravity*, Physical Review D, **44**, *2*, pp. 417–423, 1991.
8. M.A. DARIESCU, C. DARIESCU, *Robertson-Walker Branes with massless scalars and cosmological term*, Astroparticle Physics, **34**, pp. 116–120, 2010.
9. S. FERNANDO, *Schwarzschild black hole surrounded by quintessence: Null geodesics*, General Relativity and Gravitation, **44**, *7*, pp. 1857–1879, 2012.
10. L. MA, H. LÜ, *Bounds on photon spheres and shadows of charged black holes in Einstein-Gauss-Bonnet-Maxwell Gravity*, Physics Letters B, **807**, art. 135535, 2020.
11. V. CARDOSO, A. MIRANDA, E. BERTI, H. WITEK, V. ZANCHIN, *Geodesic stability, Lyapunov exponents, and quasinormal modes*, Physical Review D, **79**, *6*, art. 064016, 2009.
12. R. THARANATH, N. VARGHESE, V. KURIAKOSE, *Phase transition, quasinormal modes and hawking radiation of Schwarzschild Black Hole in quintessence field*, Modern Physics Letters A, **29**, *11*, art. 1450057, 2014.
13. B. DOLAN, *The cosmological constant and black-hole thermodynamic potentials*, Classical and Quantum Gravity, **28**, *12*, art. 125020, 2011.
14. C. DARIESCU, M.A. DARIESCU, *Relativistic particles moving around galaxy's center*, Proceedings of the Romanian Academy, Series A: Mathematics, Physics, Technical Sciences, Information Science, **23**, *1*, pp. 39–46, 2022.

Received November 14, 2022